# TARGET BUFFER ASSESSMENT FOR ACCELERATOR-DRIVEN TRANSMUTERS

**Yousry Gohar**
Argonne National Laboratory
9700 South Cass Avenue, Argonne, IL 60439, USA
gohar@anl.gov

## Abstract

Accelerator-driven transmuters use a buffer region to protect the structural and the cladding materials of the transmuter from the radiation damage caused by the high-energy spallation neutrons, to accommodate the coolant channels of the self cooled targets, and to have an insignificant effect on the neutron utilisation for the transmutation process. These functions are contradicting with respect to the buffer thickness. An extension of the target region in the axial direction (the proton beam direction) is also required to act as a neutron multiplier for the forward component of the high-energy spallation neutrons and a reflector to minimise the neutron leakage. The buffer assessment was performed as a function of its thickness with different proton energies for a self-cooled Lead-Bismuth Eutectic and a sodium-cooled tungsten targets. The analyses show that the number of generated neutrons per proton has a low sensitivity to the buffer thickness. However, the number of neutrons reaching the transmuter is significantly reduced as the buffer thickness is increased. The transmuter neutrons dominate the nuclear responses in the structural material outside the target buffer. The length of the axial target extension is determined as a function of the proton beam energy.

**Introduction**

Spallation targets are being developed worldwide to drive sub-critical transmuters. [1-5] This paper is intended to assess the buffer between the spallation target and the transmuter, and the target extension in the beam direction. The buffer is designed to perform several functions. First, it has to protect the structural and the cladding materials of the transmuter from the radiation damage caused by the high-energy spallation neutrons. Second, it has to accommodate the coolant channels of the self-cooled targets. Third, it has to have an insignificant effect on the utilisation of the generated neutrons for the transmutation process. These three functions are contradicting with respect to the buffer thickness. The target extension is designed to act as a neutron multiplier for the forward component of the high energy spallation neutrons and a reflector to minimise the neutron leakage. The buffer and the extension use the target material to simplify the mechanical design and to avoid material compatibility issues. Two different targets were considered, a self-cooled lead bismuth eutectic (LBE) target and a sodium-cooled tungsten target.

In this paper, the buffer thickness, the axial target extension, and the proton beam energy were varied. The number of neutrons generated per proton, the neutron utilisation fraction, the nuclear responses in the transmuter structure, and the helium to the atomic displacement ratio in the transmuter structure were analysed. The spallation target design of the sub-critical multiplier (SCM) of the accelerator-driven test facility (ADTF) [4-6] is used for the analyses of this paper. The ADTF is a nuclear research facility that will provide multiple testing and production capabilities. The ADTF target design is based on an LBE coaxial geometrical configuration to satisfy the SCM configuration for minimising the target space requirements and to maximise the utilisation of the target neutrons. The target is installed vertically along the SCM axis. LBE is the target material and the target coolant. Ferritic steel (HT-9, Fe-12Cr-1Mo alloy) is the structural material for the target and the transmuter. The target coolant channels and the proton beam are entered vertically from the top above the SCM. The target design shown in Figure 1 has been carefully designed to ensure flow stability and adequate cooling for the beam window and the structural material. [4] The proton beam has a uniform spatial distribution over an 8 cm circular cross-section. The beam tube has 10 cm radius to accommodate the halo current. A hemi-spherical geometry is used for the beam window, which is connected to the beam tube. The beam tube is enclosed inside two coaxial tubes to provide inlet and outlet channels for the LBE coolant. In addition, the materials (LBE and target structure) between the beam trajectory and the SCM boundary (buffer) reduce the nuclear responses in the SCM structural material. The utilisation of the LBE as a target, buffer, and coolant material does simplify the target design. The target and the beam configurations of the ADTF were adopted for the work presented in this paper.

The tungsten target replaces the LBE target of the ADTF. It uses the sodium coolant of the SCM to remove the deposited energy from the tungsten and the structural materials, which minimise the number of the ADTF coolant systems and avoid any material computability issues with SCM materials. The beam window has also a hemi-spherical geometry and it is also cooled with sodium. This target does not require the buffer to accommodate the target coolant channels, which leads to a minimum buffer thickness of 2 cm to accommodate the beam halo. In the analyses, the target region is homogenised with 65% tungsten and 35% sodium by volume.

The MCNPX code [7] was used to perform the physics analysis. Each MCNPX calculation used adequate source sampling to achieve statistical error less than 1% in any calculated parameter within one standard deviation. The paper assesses parametrically the buffer and the axial target extension. Also, recommendations are defined to maximise the neutron utilisation and to protect the structural material outside the target buffer from the high-energy neutrons.

**Neutron yield**

As a first step, the neutron yield analysis of the LBE target was performed as a function of the buffer thickness for 600 and 1 000 MeV proton energies. The cross-section areas required for the inlet and the outlet coolant channels define the minimum buffer thickness, which is 7 cm for the 5 MW proton beam. [4] Figure 2 show that the number of generated neutrons per proton has low sensitivity to the buffer thickness. It has a very broad peak at a buffer thickness of ~40 cm. The peak value is ~1.14 times the value obtained with the 7 cm minimum buffer thickness. The high-energy spallation neutrons multiply through (n,xn) interactions with LBE causing this increase and the very low parasitic neutron absorption of LBE helps maintaining a net increase in the neutron yield. The number of neutrons per proton is more than doubled as the proton energy increases from 600 to 1 000 MeV, as shown in Figure 2. This result shows that the use of high-energy protons is beneficial for enhancing the neutron yield. However, the neutron fraction with energy above 20 MeV is not sensitive to the proton energy and it is in the range of 2 to 6% of the total generated neutrons. The exact value depends on the buffer thickness as shown in Figure 2.

In order to define the buffer thickness, the number of neutrons reaching the sub-critical multiplier for performing transmutation (utilised neutrons) per proton is considered. This number is significantly reduced as the buffer thickness increases. For the 600 MeV proton beam, the number drops from 7.8 neutrons per proton with 7 cm buffer to 3.3 neutrons per proton with 40 cm buffer. The axial neutron leakage is increased faster than the total neutron yield increase as the buffer thickness increases. This requires the target to reduce the buffer thickness as much as possible. The neutron utilisation fraction is defined as the neutron fraction of the total generated neutrons that does not leave the target region in the beam direction because these neutrons have the opportunity to perform material transmutation. This fraction is plotted in Figure 3 for the 600 and 1 000 MeV protons, which is not sensitive to the proton energy.

The required target length to stop the proton beam is obtained from the axial energy deposition profile. The energy deposition profile is shown in Figure 4 as a function of the distance along the beam axis for the 600 and 1 000 MeV protons. The required target length is ~32 and ~64 cm to stop the 600 and 1 000 MeV protons, respectively. The peak energy deposition is 20.8 and 25 $W/cm^3/(\mu A/cm^2)$ at 1.65 and 2.65 cm from the LBE surface for both energies, respectively. Engineering and neutron yield considerations require extending the target length. The thermal-hydraulics analyses require a small target extension to insure the flow stability of the lead-bismuth eutectic in the target and the appropriate temperature distribution in the target structure, [4] which represents the minimum extension length. The neutron yield was analysed as a function of the target length for 600 and 1 000 MeV protons. Figures 5 and 6 give the total and the utilised neutrons in terms of neutrons per proton normalised to the results of the 80 cm target length. The results show that the neutron yield reaches saturation as the target length increases. For the 600 MeV proton beam, a target length of 38 cm (6 cm extension) generates ~98% of the total possible neutrons and utilises ~90% of the utilised neutrons of the 80 cm target length. However, the 1 000 MeV proton beam does not require any extension as can be seen from the results of Figure 6. The thermal-hydraulics defines the target extension length for the target with the 1 000 MeV proton beam.

Similar analyses were carried out for the tungsten target. First the analyses used pure tungsten material without the sodium coolant to define the performance of the tungsten target material. The neutron yield was analysed for the tungsten material as a function of the buffer thickness for 600 and 1 000 MeV proton energies. The minimum buffer thickness is 2 cm to accommodate the beam halo. Figure 7 shows the obtained results, which show different behaviour from the LBE results. The neutron yield decreases as the buffer thickness increases because the neutron absorption in the tungsten is greater than the neutron multiplication through (n,xn) interactions for 600 and 1 000 MeV

proton energies. The tungsten buffer is more efficient in reducing the neutron fraction with energy above 20 MeV relative to the LBE buffer as shown in Figure 7. Tungsten has higher inelastic scattering cross-section than LBE that slows down the high energy component of the neutron spectrum. The tungsten buffer has also a strong negative effect on the neutron utilisation for the two proton energies under consideration. The neutron utilisation factor of the 600 MeV proton beam is less than that of 1 000 MeV for the same buffer thickness as shown in Figure 8. The neutrons generated from the 600 MeV proton interactions occur over shorter section of the target relative to 1 000 MeV case as can be seen from Figure 9, which results in more neutron interactions inside the target including parasitic absorption interactions. The required tungsten target length is less than half of the LBE target for the same proton energy as can be seen by comparing the results of Figures 4 and 9. Also, the peak energy deposition value in tungsten is more than double that of LBE.

In the tungsten target, the sodium coolant is used to remove the energy deposition. The tungsten material volume fraction is 65%, which extends the target length by a factor of 1.54 to stop the proton beam. The buffer analyses were repeated to account for the sodium coolant and the neutron yield results are shown in Figure 10. The sodium coolant reduces the neutron yield and changes the effect of the buffer thickness on the neutron yield as shown in Figure 10. The neutron yield reaches a peak at about 6.5 cm thick buffer. The peak value has ~2.6% more neutrons compared to the neutron yield with 2 cm buffer required for the beam halo. The sodium coolant increases the proton scattering and reduces the slowing down characteristics of the target, which causes the positive effect from increasing the buffer thickness with respect to the neutron yield. However, the neutron utilisation factor is reduced as the buffer thickness increase, which calls also for the use of the smallest buffer thickness.

**Nuclear responses in the transmuter structural material**

The nuclear responses in the structural material outside the LBE target buffer are analysed as a function of the distance along the outer buffer boundary measured from the top surface of the 100 MW SCM fuel for different buffer thicknesses with 5 MW beam power and 600 MeV protons. For a small buffer thickness, the results show that the peak values of the different nuclear responses occur near the SCM midplane. As the buffer thickness increases, the nuclear responses are reduced and the peak values of the gas production, helium and hydrogen, shift to the top section of the sub-critical multiplier. On the other hand, the maximum atomic displacement stays at the SCM midplane. This means that the SCM fission neutrons are causing most of the nuclear responses for the small buffer thickness. For the SCM with a constant total power of 100 MW, as the buffer thickness increases, the SCM volume increases to compensate for the increased neutron leakage. Therefore, the SCM average power density and the nuclear responses, which are dominated by the fission neutrons, are decreased. This explains the change in the gas production distribution where the contribution from the target neutrons are noticeable at the top of the target and decrease along the target length for the large buffer sizes. However, the atomic displacement distribution maintains the peak value at the SCM midplane because the SCM fission neutrons is the main contributor.

The nuclear responses at the SCM midplane are shown as a function of the reciprocal of the outer buffer radius in Figure 11. The results show a good linear fit because the fission neutrons dominate the reaction rates at the SCM boundary. The other important parameter for the structural material performance is the helium to the atomic displacement ratio, which is in the range of 0.1 to 0.3. This ratio is ~0.26 for HT-9 in a typical fast reactor spectrum. For the LBE target, these results show that the 7 cm buffer thickness protects the structural material from the nuclear responses caused by the high-energy neutrons and utilises most of the neutrons for driving the sub-critical multiplier. The lifetime of the SCM structural material will depend on the operating temperature, the nuclear response values, and the mechanical loading conditions similar to the fast fission reactors.

Similar analyses were performed for the sodium-cooled tungsten target. The total SCM power is maintained at 100 MW with 5 MW beam power using 600 MeV protons. The results show similar behaviour to the results from the LBE target. For the same buffer thickness, the nuclear responses, the atomic displacement and the gas production from the sodium-cooled tungsten target are lower than the corresponding values from the LBE target. The difference in the inelastic scattering cross-section of target materials is responsible for the difference in the nuclear responses. Figure 12 shows the nuclear responses at the SCM midplane as a function of the reciprocal of the outer buffer radius, which have a good linear fit. The helium to the atomic displacement ratio is about twice the corresponding value for the LBE target without buffer. As the buffer thickness increases, the difference between the two ratios is reduced. At 18 cm buffer thickness, this ratio is ~0.1 for both targets.

## Conclusions

Several conclusions were obtained from this paper, which contribute to the development of the spallation targets for driving sub-critical systems. The analyses addressed the neutron yield, the neutron utilisation fraction, the nuclear responses in the structural material outside the target buffer, the buffer size, and the axial target extension for lead-bismuth eutectic and sodium-cooled tungsten targets. The main conclusions can be summarised as follows:

1.  The neutron yield increases with the proton energy. The high-energy neutron fraction (E >20 MeV) is not sensitive to the proton energy and it is less than 6% of the total generated neutrons.

2.  For lead-bismuth eutectic and sodium-cooled tungsten targets, the neutron yield is not sensitive to the buffer thickness. The neutron utilisation factor decreases fast as the buffer thickness increases.

3.  The thermal hydraulics analyses define the minimum buffer thickness for the lead-bismuth eutectic targets, which is ~7 cm thick for the target with 5 MW of beam power. For the sodium-cooled tungsten target, the beam halo defines the minimum buffer thickness, which is ~2 cm thick. The physics analyses calls for reducing the buffer thickness for both targets as much as possible.

4.  For the Lead-bismuth eutectic target, the required axial target extension is a function of the proton energy. A 6 cm target extension is needed for the 600 MeV protons. As the proton energy increases to 1 000 MeV, no extension is needed. At this proton energy, the thermal-hydraulics analyses define the required extension.

5.  The nuclear responses in the structural material outside the target buffer are dominated by the transmuter neutrons. Consequently, the nuclear responses at the SCM midplane show a good linear fit with the reciprocal of the outer buffer radius for a constant transmuter power.

6.  The helium to the atomic displacement ratio is similar to the observed value for fast reactor system. For small buffer thicknesses, the tungsten target exhibits relatively higher ratio relative the LBE target.

## Acknowledgements

# REFERENCES

[1]  A. Dedoul, B. Gromov, E. Yefimov, E. Zemskov, K. Ivanov, M. Leonchuk. Yu. Orlov, D. Pankratov, Z. Sivack, V. Troyanov, N. Khaveyev, V. Chitaykin, V. Chekunov, N. Klimov, M. Koulikov, V. Stepanov, T. Kitano, M. Ono (2001), *Conceptual Design of Molten Lead-Bismuth Target Complex of Integral Type for ADS*, Accelerator Applications – Accelerator-driven Transmutation Technology and Applications 01 (AccApp-ADTTA'01), Reno, Nevada, November.

[2]  Joachim U. Knebel, Jean-Christophe Klein, Dominique Gorse, Pietro Agostini, Friedrich Gröschel, Peter Kupschus, Thomas Kirchner, Jean-Bernard Vogt (2001), *MEGAPIE-TEST: A European Project on Spallation Target Testing*, Accelerator Applications – Accelerator-driven Transmutation Technology and Applications 01 (AccApp-ADTTA'01), Reno, Nevada, November.

[3]  A. Dedoul, S. Grishakov, Ye. Yefimov, Ye. Zemskov, M. Leonchuk, D. Pankratov, D. Rachkova, Z. Sivak, V. Chitaykin, V. Chekunov, S. Sidorkin, F. Perekrestenko, V. Stepanov, N. Klimov, M. Kulikov (2001), *Concept of Lead-Bismuth Liquid Metal Target for Proton Accelerator of Moscow Meson Plant*, Accelerator Applications – Accelerator-driven Transmutation Technology and Applications 01 (AccApp-ADTTA'01), Reno, Nevada, November.

[4]  Yousry Gohar, Phillip J. Finck, Lubomir Krajtl, Joseph E. Herceg, W. David Pointer, James Saiveau, Tanju Sofu, Albert L. Hanson, Michael Todosow, Maria Koploy and Panto Mijatovic (2002), *Lead-Bismuth Target Design for the Sub-critical Multiplier (SCM) of the Accelerator-driven Test Facility (ADTF)*, Argonne National Laboratory Report, ANL/TD/02-01.

[5]  Y. Gohar, J. Herceg, L Krajtl, D. Pointer, J. Saiveau, T. Sofu and P. Finck (2001), *Lead-Bismuth-Eutectic Spallation Neutron Source for Nuclear Transmuter*, Accelerator Applications – Accelerator-driven Transmutation Technology and Applications 01 (AccApp-ADTTA'01), Reno, Nevada, November.

[6]  Yousry Gohar, Phillip Finck, Joseph Herceg, Lubomir Krajtl, W. David Pointer, James Saiveau, Tanju Sofu, Albert Hanson and Michael Todosow, Maria Koploy, Panto Mijatovic (2002), *Lead-Bismuth Target Design for Transmutation Reactors*, PHYSOR 2002, International Conference on the New Frontiers of Nuclear Technology: Reactor Physics, Safety and High-Performance Computing, Seoul, Korea, October 7-10.

[7]  MCNPX Team (2002), *MCNPX Version 2.4.j*, Los Alamos National Laboratory, LA-UR-02 2127, March 25.
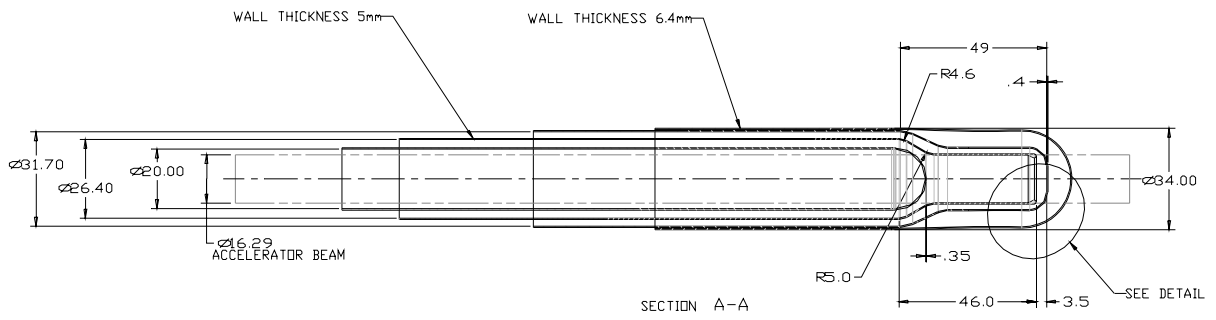
Figure 1.  **Lead-bismuth eutectic target design**



Figure 2.  **Number of generated neutrons per proton as a function of the buffer thickness for the LBE target for different proton energies**
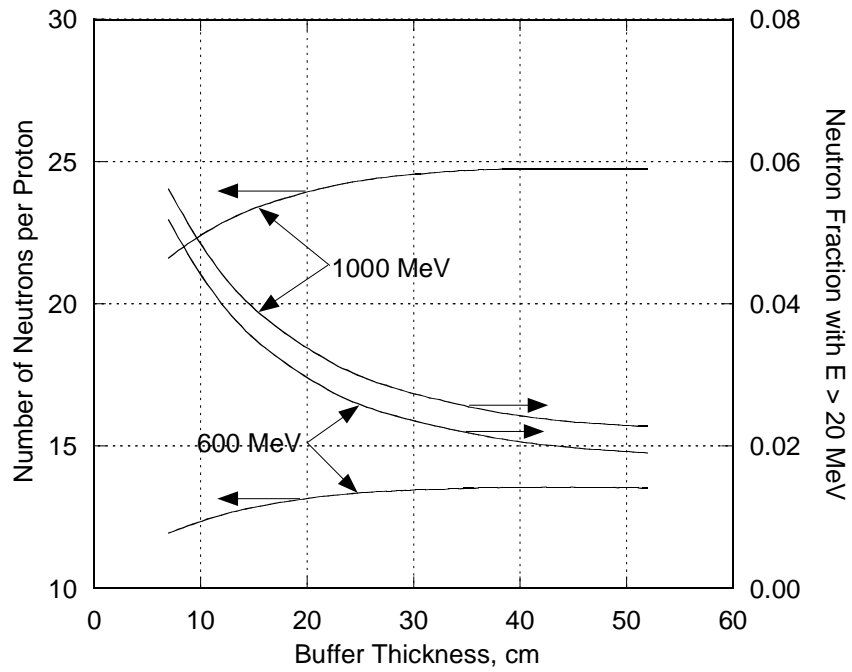
Figure 3. **Neutron yield and neutron utilisation fraction as a function of the buffer thickness for LBE target with 600 and 1 000 MeV proton beams**
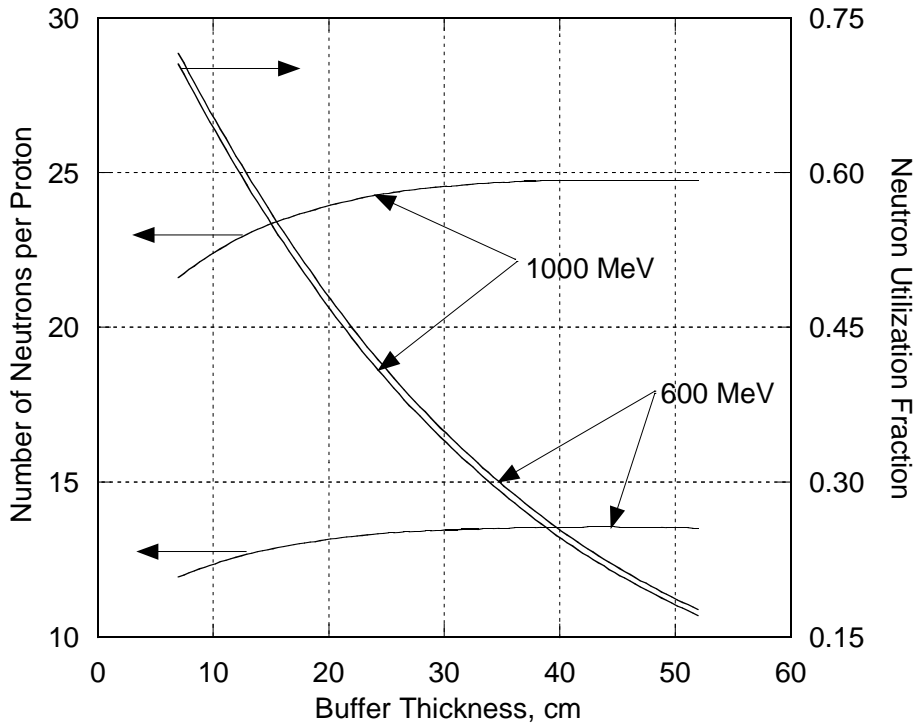


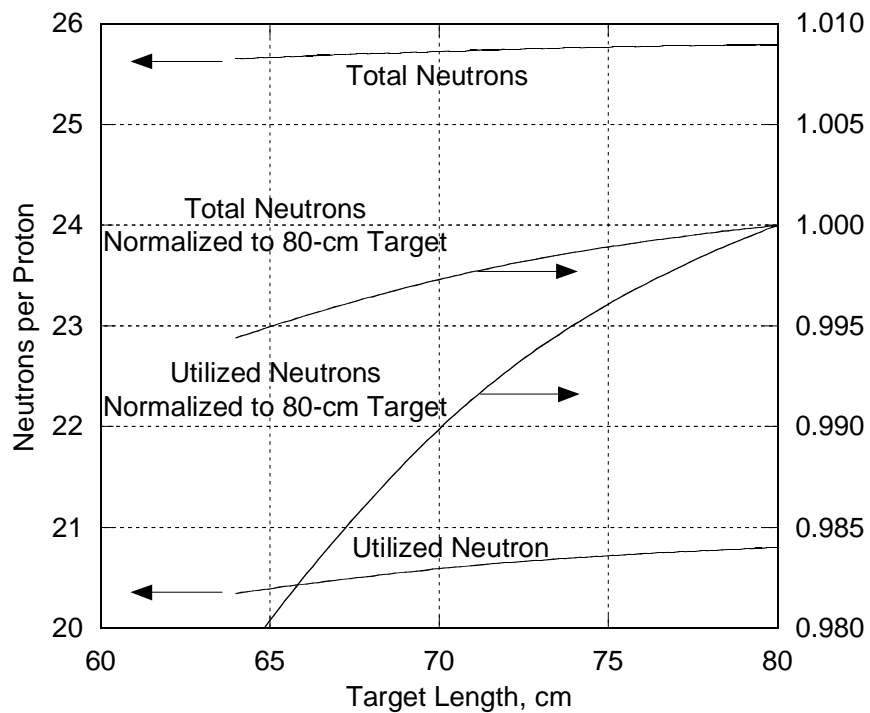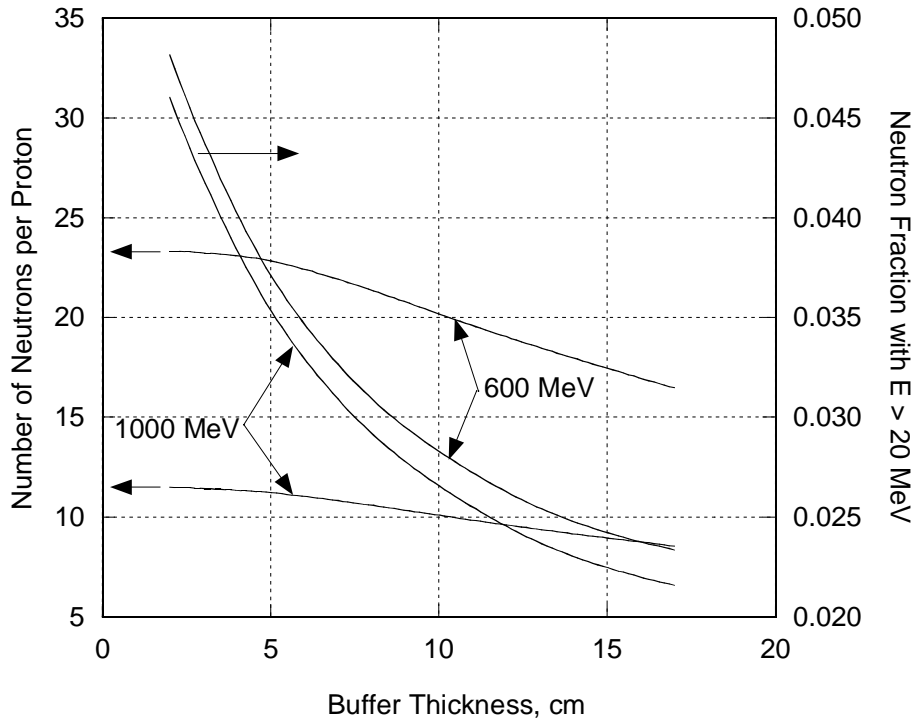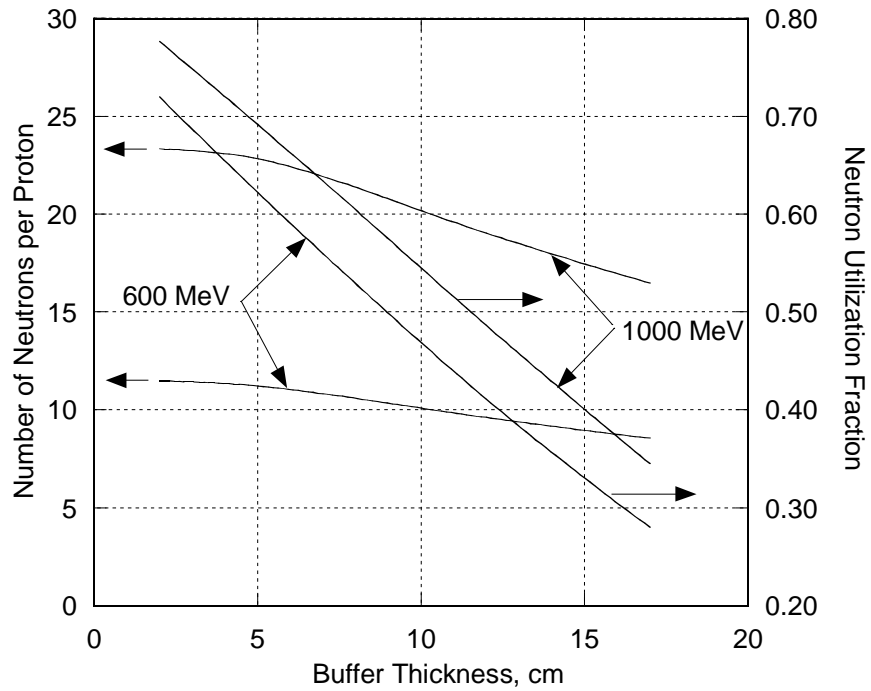Figure 4. **Spatial energy deposition in the lead-bismuth eutectic for different proton energies with a uniform beam distribution normalised to the proton beam current density**
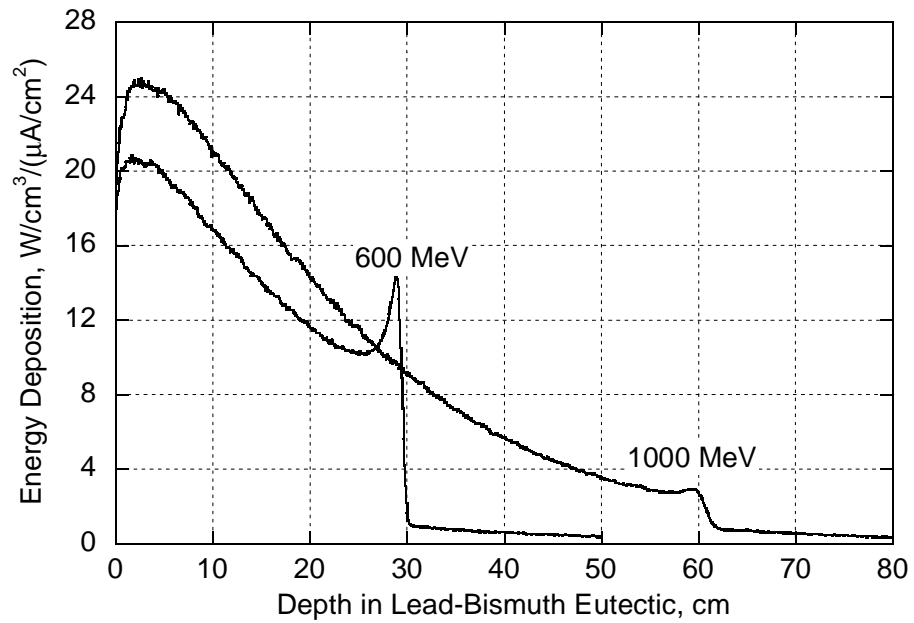
Figure 5. **Number of generated and utilised neutrons per 600 MeV proton as a function of the LBE target length**
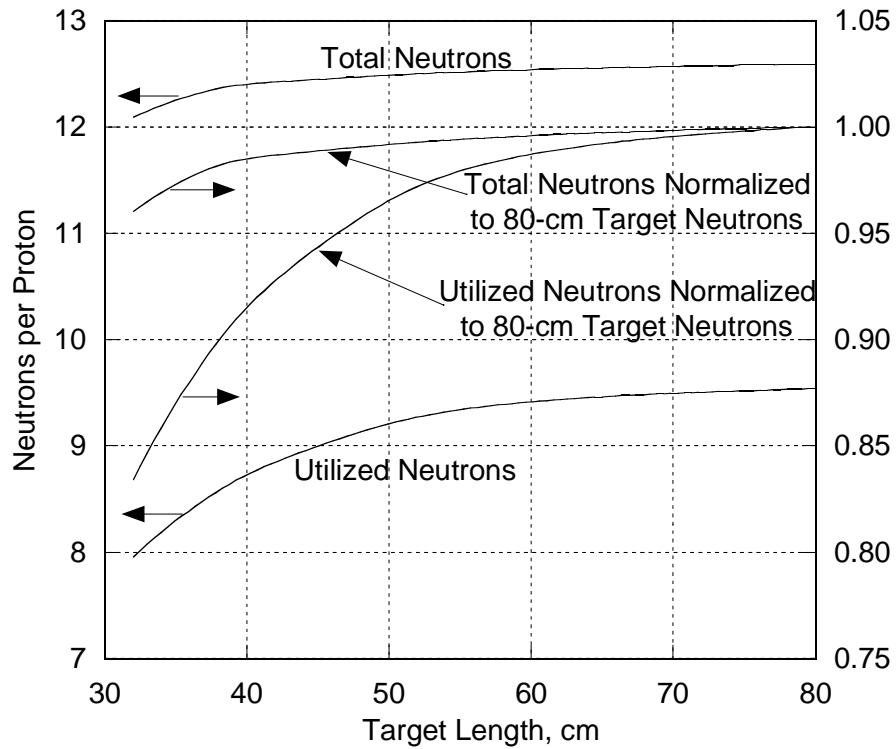


Figure 6. **Number of generated and utilised neutrons per 1 000 MeV proton as a function of the LBE target length**



1021

Figure 7. **Number of generated neutrons per proton as a function of the buffer thickness for the tungsten target for different proton energy**



Figure 8. **Neutron yield and neutron utilisation fraction as a function of the buffer thickness for the tungsten target with 600 and 1 000 MeV proton beams**

Figure 9. **Spatial energy deposition in the tungsten material for different proton energies with a uniform beam distribution normalised to the proton beam current density**
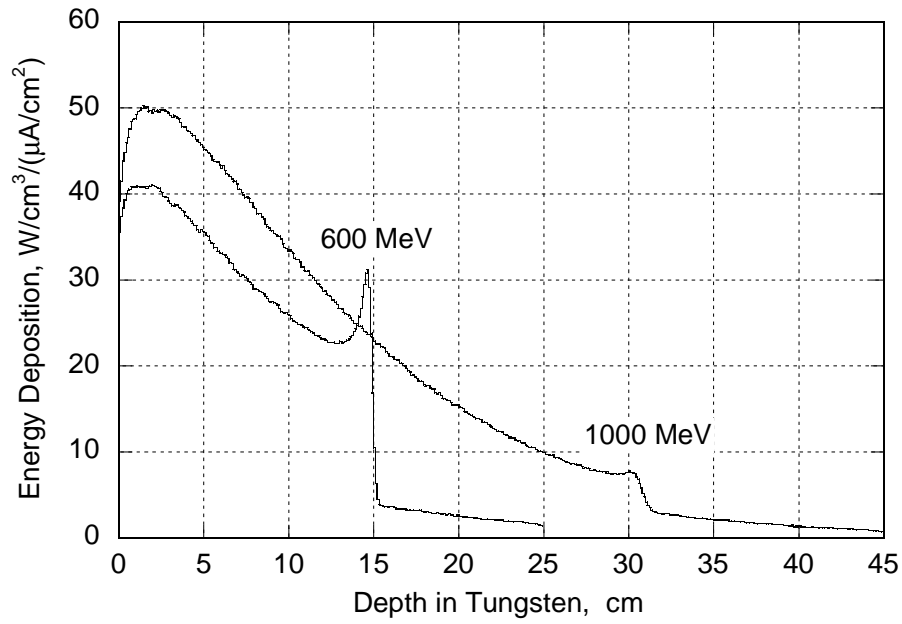


Figure 10. **Number of generated neutrons per proton as a function of the buffer thickness for the sodium-cooled tungsten target with the 600 MeV proton beam**
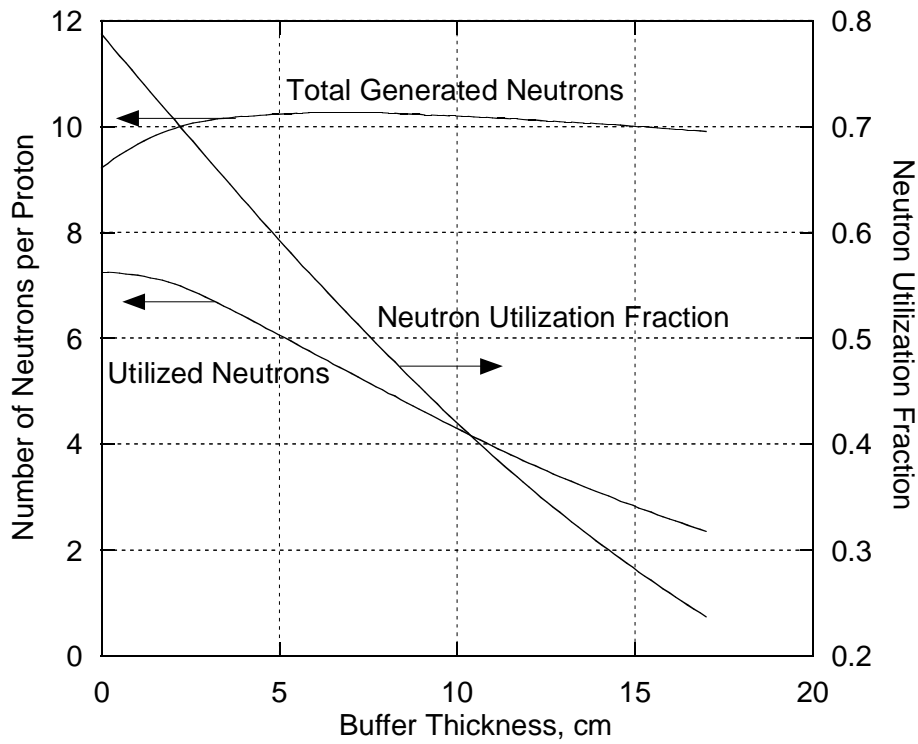
Figure 11. **Midplane nuclear responses in the SCM structural material as a function of the reciprocal of the outer buffer radius for the LBE target with 600 MeV proton beam**
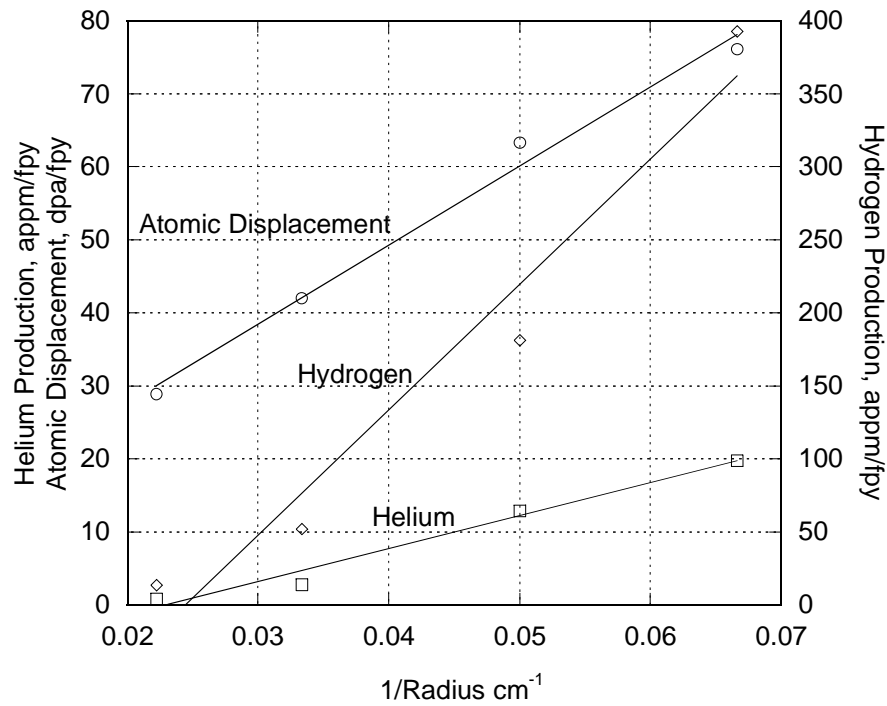


Figure 12. **Midplane nuclear responses in the SCM structural material as a function of the reciprocal of the outer buffer radius for the sodium-cooled tungsten target with 600 MeV proton beam**